Electronic Supplementary Material (ESI) for CrystEngComm.
This journal is © The Royal Society of Chemistry 2016

Supporting Information for

"^{35}Cl Solid-State NMR for the Identification of HCl Pharmaceuticals and their Polymorphs in Bulk and Dosage Forms"

Andrew M. Namespetra, Marcel P. Hildebrand, Anthony R. Sandre, David A. Hirsh, Hiyam Hamaed, Jeremy M. Rawson and Robert W. Schurko†,*

University of Windsor, Department of Chemistry and Biochemistry, Windsor, Ontario, Canada N9B 3P4

*Author to whom correspondence should be addressed. E-mail: rschurko@uwindsor.ca; Web: http://www.uwindsor.ca/schurko; Tel: (519) 253-3000 x3548; Fax: (519) 973-7098

Table of Contents:

Table S1. Weight percentage of chlorine in bulk samples

API	Chemical Formula	Molecular weight (g mol^{-1})	Purity of sample [a] (%)	Percent weight of Cl in bulk sample [b]
Metf	$C_4H_{12}N_5Cl$	215.72	99	21.2
Diph	$C_{17}H_{22}NOCl$	291.817	98	11.9
Nica	$C_{26}H_{30}N_3O_6Cl$	515.986	98	6.73
Mexi	$C_{11}H_{18}NOCl$	215.72	98	16.1
Isox	$C_{18}H_{24}NO_3Cl$	337.82	98	10.3

[a] The purity of the sample was indicated by Sigma-Aldrich upon purchase.
[b] The percent mass of Cl in the sample was calculated as follows:

$$\%\ \text{weight of Cl} = \frac{\text{moles Cl}}{\text{moles API}} \times \frac{\text{MW of Cl}}{\text{MW of API}} \times \text{purity of sample} \times 100\ \%$$

Table S2. Weight percentage of chlorine in dosage forms

API	Tablet Mass (g)	Dose of Active Ingredient (g)	Weight % of Active Ingredient [a]	Mass of Cl in Dose of API (g)	Weight % of Cl in dosage form [b]	Mass of Cl (bulk:dose)
Metf	0.660	0.5	75.7	0.10702	16.22	1.31
Diph	0.408	0.025	6.12	0.00304	0.74	16.1
Nica	0.162	0.02	12.3	0.00137	0.84	8.02
Mexi	0.317	0.2	63.1	0.03287	10.37	1.55
Isox	0.202	0.01	4.95	0.00105	0.52	19.8

[a] The percent weight of the active ingredient within the dosage form was calculated as follows:

$$\%\ \text{weight of API} = \frac{\text{Dose of active ingredient}}{\text{Tablet weight}} \times 100\ \%$$

[b] The percent weight of Cl within the dosage form was calculated as follows:

$$\%\ \text{weight of Cl} = \left[\frac{\left(\frac{\text{Stoichiometric MW of Cl in API}}{\text{MW of API}}\right) \times \text{Dose of API}}{\text{Tablet mass}}\right] \times 100\ \%$$

Table S3. ^{35}Cl SSNMR acquisition parameters for static Hahn-echo experiments at 9.4 T

	Metf	
	Bulk	Tablet
Spectrometer frequency (MHz)	39.165	39.165
Number of sub-spectra acquired	1	1
Transmitter offset per piece (kHz)	----	----
Number of scans per sub-spectrum	320	640
Experimental time per sub-spectrum (h)	0.9	1.8
Recycle delay (s)	10	10
Dwell (μs)	5.0	5.0
Spectral width (kHz)	200	200
Acquisition length (number of points)	1024	1024
90° pulse width [π/2] (μs)	2.1	2.1
180° pulse width [π] (μs)	4.2	4.2
^{1}H decoupling field (kHz)	31.25	31.25

Table S4. ^{35}Cl SSNMR acquisition parameters for static WURST-QCPMG experiments at 9.4 T

	Diph		Nica		Mexi	Isox		
	Bulk	Tablet	Bulk	Capsule	Capsule	Isox-I	Isox-II	Tablet
Number of scans	57197	107488	5120	50216	157527	8409	43360	122496
Experimental time (h)	7.9	14.9	0.7	13.9	21.9	1.2	6.0	17.0
Recycle delay (s)	0.5	0.5	0.5	1.0	0.5	0.5	0.5	0.5
Meiboom-Gill loops [N] (i.e., Number of echoes)	1	1	36	90	1	35	80	35
Real points per loop (i.e., points per echo)	512	512	150	60	512	200	200	200
Echo length (ms)	1.0	1.0	0.30	0.12	1.0	0.4	0.16	0.4
Dwell (μs)	2.0	2.0	2.0	2.0	2.0	2.0	2.0	2.0
Spectral width (kHz)	500	500	500	500	500	500	500	500
Acquisition length (number of points)	512	512	5400	5400	512	7000	16000	7000
Acquisition time (ms)	1.0	1.0	10.8	10.8	1.0	14.0	32.0	14.0
WURST pulse width (μs)	100	100	50	50	100	50	50	50
Sweep of WURST pulse (kHz)	400	400	500	500	400	500	500	500
Sweep rate of WURST pulse (MHz/ms)	4	4	10	10	4	10	10	10

Table S5. ^{35}Cl SSNMR acquisition parameters for BRAIN-CP/WCPMG experiments at 9.4 T

	Nica		Isox		
	Bulk	Capsule	Isox-I	Isox-II	Tablet
Number of scans	512	10044	700	3612	10208
Experimental time (h)	0.7	13.9	1.2	6.0	17.0
Recycle delay (s)	5.0	5.0	6.0	6.0	6.0
^{1}H $\pi/2$ pulse width (μs)	5.0	5.0	5.0	5.0	5.0
Contact time (ms)	20	20	25	25	20
^{1}H Hartmann-Hahn matching field (kHz)	59.1	59.1	59.1	59.1	59.1
^{35}Cl Hartmann-Hahn matching field (kHz)	9.58	9.58	6.76	6.76	6.76
Meiboom-Gill loops [N] (i.e., Number of echoes)	36	90	35	80	35
Real points per loop (i.e., Points per echo)	150	60	200	200	200
Dwell (μs)	2.0	2.0	2.0	2.0	2.0
Spectral width (kHz)	500	500	500	500	500
Acquisition length (number of points)	5400	5400	7000	16000	7000
Sweep of WURST contact pulse (kHz)	200	200	200	200	200
^{35}Cl WURST pulse width (μs)	50	50	50	50	50
Sweep range of ^{35}Cl WURST pulse (kHz)	500	500	500	500	500
^{1}H decoupling field (kHz)	82.0	82.0	82.0	82.0	82.0

Table S6. ^{35}Cl SSNMR acquisition parameters for static BRAIN-CP/echo experiments at 9.4 T

	Metf	
	Bulk	Tablet
Number of scans	80	160
Experimental time (h)	0.9	1.8
Recycle delay (s)	40	40
^{1}H $\pi/2$ pulse width (μs)	5.0	5.0
Contact time (ms)	40	40
^{1}H Hartmann-Hahn matching field (kHz)	125	125
^{35}Cl Hartmann-Hahn matching field (kHz)	6.76	6.76
Real points per loop (i.e., Points per echo)	1024	1024
Echo length (ms)	4.1	4.1
Dwell (μs)	4.0	4.0
Spectral width (kHz)	250	250
Acquisition length (number of points)	1024	1024
Acquisition time (ms)	4.1	4.1
Sweep range of WURST contact pulse (kHz)	100	100
^{35}Cl $\pi/2$ pulse width (μs)	2.1	2.1
^{1}H decoupling field (kHz)	59.1	59.1

Table S7. ^{35}Cl SSNMR acquisition parameters for static Hahn-echo experiments at 21.1 T on Diph, Mexi, and Metf

	Diph		Mexi			Metf	
	Bulk	Tablet	Mexi-I	Mexi-II	Tablet	Bulk	Tablet
Number of scans	206848	2500608	36864	20480	450560	288	5040
Experimental time (h)	1.1	17.8	5.1	2.8	62.5	0.8	14.0
Recycle delay (s)	0.02	0.02	0.5	0.5	0.5	10	10
Dwell (μs)	2.0	2.0	2.0	2.0	2.0	1.4	1.4
Spectral width (kHz)	250	250	250	250	250	357.1	357.1
Acquisition length (number of points)	2048	2048	1024	1024	1024	8192	8192
90° pulse width [π/2] (μs)	3.0	3.0	3.0	3.0	3.0	1.9	1.9
180° pulse width [π] (μs)	6.0	6.0	6.0	6.0	6.0	3.8	3.8

Table S8. ^{35}Cl SSNMR acquisition parameters for static CPMG experiments at 21.1 T on Isox

	Isox		
	Isox-I	Isox-II	Tablet
Number of scans	63600	61696	215552
Experimental time (h)	17.7	17.1	59.8
Recycle delay (s)	1.0	1.0	1.0
Meiboom-Gill loops [N] (i.e., Number of echoes)	20	20	20
Real points per loop (i.e., Points per echo)	256	256	256
Echo length (ms)	1.024	1.024	1.024
Dwell (μs)	2	2	2
Spectral width (kHz)	250	250	250

Table S9. ^{35}Cl SSNMR acquisition parameters for static WURST-QCPMG experiments at 21.1 T

	Nica	
	Bulk	Capsule
Number of scans	5088	4736
Experimental time (h)	0.71	0.66
Recycle delay (s)	0.5	0.5
Meiboom-Gill loops [N] (i.e., Number of echoes)	25	45
Real points per loop (i.e., Points per echo)	600	304
Echo length (ms)	0.75	0.38
Dwell (μs)	1.25	1.25
Spectral width (kHz)	400	400
Acquisition length (number of points)	17024	17124
Acquisition time (ms)	21.33	21.45
WURST pulse width (μs)	50	50
Sweep range of WURST pulse (kHz)	1000	1000
Sweep rate of WURST pulse (MHz/ms)	20	20

Table S10. ^{35}Cl SSNMR acquisition parameters for MAS experiments at 21.1 T

	Diph		Metf		Nica	
	Bulk	Tablet	Bulk	Tablet	Bulk	Capsule
Pulse sequence	Hahn echo	DFS decay	Hahn echo	Hahn echo	DFS decay	DFS decay
Number of scans	3920	11600	1024	1792	3904	124928
Experimental time (h)	0.54	1.6	1.42	2.48	0.54	17.4
Recycle delay (s)	0.5	0.5	5	5	0.5	0.5
Dwell (μs)	2.5	2.5	5	5	2.5	2.5
Spectral width (kHz)	200	200	100	100	200	200
Acquisition length (number of points)	2048	2048	2048	2048	2048	2048
90° pulse width [π/2] (μs)	2.88	2.88	3.0	3.0	2.88	2.88
DFS pulse width (μs)	N/A	1000	N/A	N/A	1000	1000
Starting frequency of sweep (kHz)	N/A	200	N/A	N/A	200	200
Starting frequency of sweep (kHz)	N/A	1500	N/A	N/A	1500	1500
Spinning speed (kHz)	22	22	18	18	22	22

Table S11. SSNMR acquisition parameters for $^{1}H \rightarrow ^{13}C$ VACP/MAS experiments at 9.4 T

	Diph		Metf	
	Bulk	Tablet	Bulk	Tablet
Number of scans	4080	10731	3554	4892
Experimental time (h)	4.0	13.4	3.5	4.8
Recycle delay (s)	3.5	4.5	3.5	3.5
Contact time (ms)	6.0	2.0	2.5	2.5
^{1}H Hartmann-Hahn matching field (kHz)	49.9	49.9	59.1	59.1
^{1}H $\pi/2$ pulse width (μs)	2.9	3.0	5.5	5.5
Dwell (μs)	20	20	16.66	16.66
Spectral width (kHz)	50	50	60.02	60.02
Acquisition length (number of points)	2048	1024	1024	1024
^{1}H decoupling field (kHz)	39.3	39.3	39.3	39.3
Spinning speed (kHz)	10	10	8	8

Table S12. SSNMR acquisition parameters for $^{1}H \rightarrow ^{13}C$ VACP/MAS experiments of Isox and Mexi samples at 9.4 T

	Isox				Mexi			
	Isox-I[a]	Isox-II[a]	Isox tablet		Mexi-I[a]	Mexi-II[a]	Mexi-III[a]	Mexi capsule
Number of scans	8500	9245	39588	23220	40000	40000	16000	40000
Experimental time (h)	4.7	5.1	22.0	12.9	11.1	11.1	4.4	11.1
Recycle delay (s)	2.0	2.0	2.0	2.0	1.0	1.0	1.0	1.0
Contact time (ms)	4.0	4.0	10.0	4.0	1.5	1.0	5.0	1.0
^{1}H Hartmann-Hahn matching field (kHz)	57.9	57.9	38.5	38.5	54.4	54.4	54.4	38.5
^{1}H $\pi/2$ pulse width (μs)	2.4	2.4	3.2	3.2	2.4	2.4	2.4	3.2
Dwell (μs)	20	20	20	20	20	20	20	20
Spectral width (kHz)	50	50	50	50	50	50	50	50
Acquisition length (number of points)	1024	1024	1024	1024	1024	1024	1024	1024
^{1}H decoupling field (kHz)	62.5	62.5	38.5	38.5	62.5	62.5	62.5	26.8
Spinning speed (kHz)	13	13	13	13	9.5	9.5	9.5	9.5

[a] Data reported by Hildebrand *et al*.[1]

Table S13. SSNMR acquisition parameters for $^{1}H \rightarrow ^{13}C$ VACP/MAS experiments at 11.7 T

	Nica	
	Bulk	Capsule
Number of scans	8144	64800
Experimental time (h)	11.3	18
Recycle delay (s)	5.0	5.0
Contact time (ms)	7.0	2.5
^{1}H Hartmann-Hahn matching fields (kHz)	83.3	83.3
^{1}H $\pi/2$ pulse width (μs)	3.0	3.0
Dwell (μs)	18.133	18.133
Spectral width (kHz)	27.57	27.57
Acquisition length (number of points)	1006	512
^{1}H decoupling field (kHz)	83.3	83.3
Spinning speed (Hz)	12	12

Table S14. Selected crystallographic and data collection parameters for Mexi-II.

Empirical Formula	$C_{11}H_{17}NO$, HCl
MW (g/mol)	215.71
Crystal System	Orthorhombic
Space Group	*Pbcn*
a (Å)	35.116(2)
b (Å)	7.7402(5)
c (Å)	9.1539(5)
α (°)	90
β (°)	90
γ (°)	90
V (Å^3)	2488.1(3)
Z	8
D_c (Mg/m^3)	1.152
Absorption coefficient, μ (mm^{-1})	0.279
F(000)	928
Crystal size (mm)	0.40 × 0.18 × 0 ×.06
Crystal color and habit	colourless plate
θ range for data collection	2.69 – 25.0
Reflections collected	30104
Independent reflections	2192
Observed reflections [$I > 2\sigma(I)$]	2166
R(int)	0.0344
Data/restraints/parameters	2192/0/131
Goodness of fit on F^2	1.452
Final R indices [$I > 2\sigma(I)$]	$R_1 = 0.0577$, $wR_2 = 0.1075$
Final R indices [all data]	$R_1 = 0.0585$, $wR_2 = 0.1078$
Residual electron density	+0.23/−0.34

Table S15. Signal-to-noise in ^{35}Cl SSNMR spectra for DE and CP experiments.

API	Sample	Pulse Sequence	Exp. Time (h)	Number of scans	S/N	Processing parameters
Metf	Bulk	BRAIN-CP/Echo	0.9	80	34.5	DC correction, FT, MC
		Hahn echo	0.9	320	4.4	DC, LS 29, FT, zero order phasing
	Tablet	BRAIN-CP echo	1.8	160	36.7	DC correction, FT, MC
		Hahn echo	1.8	640	6.3	DC, LS 29, FT, zero order phasing
Nica	Bulk	BRAIN-CP/WQCPMG	0.7	512	41.2	FT, MC
		WURST-QCPMG	0.7	5120	16.2	FT, MC
	Capsule	BRAIN-CP/WQCPMG	13.9	10044	25.4	FT, MC
		WURST-QCPMG	13.9	50216	12.0	FT, MC
Isox	Isox-I	BRAIN-CP/WQCPMG	1.2	1051	198.9	FT, MC
		WURST-QCPMG	1.2	8409	58.4	FT, MC
	Isox-II	BRAIN-CP/WQCPMG	1.5	904	59.3	FT, MC
		WURST-QCPMG	1.5	10840	42.0	FT, MC
	Tablet	BRAIN-CP/WQCPMG	17.0	10208	28.6	FT, MC
		WURST-QCPMG	17.0	122496	9.8	FT, MC

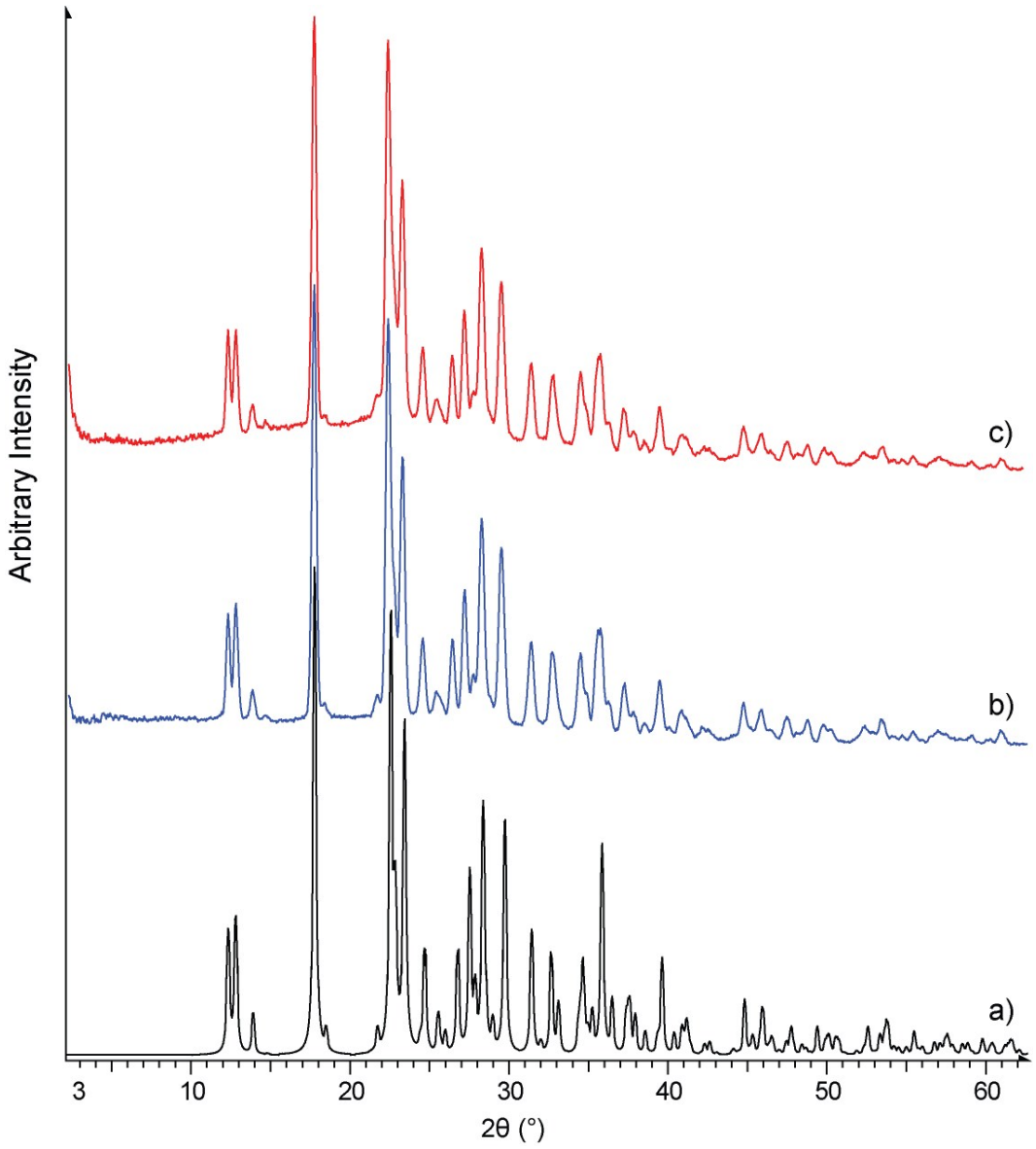

Figure S1. The (a) simulated PXRD pattern of the crystal structure of Metf,[2] (b) experimental pXRD pattern of bulk Metf, and (c) experimental PXRD pattern of Metf tablet.

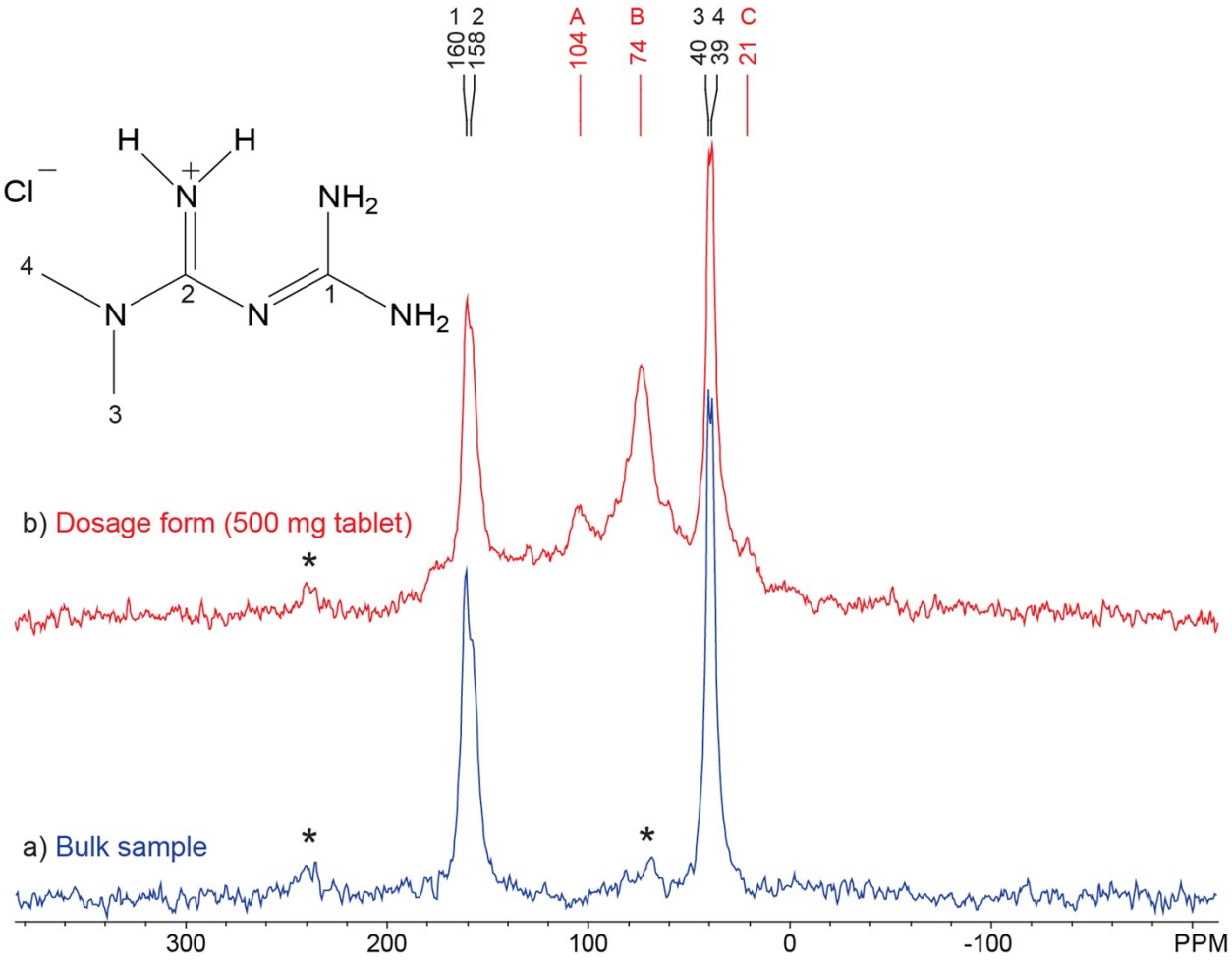

Figure S2. ^{1}H-^{13}C{^{1}H VACP/MAS SSNMR spectra of (a) Metf (bulk) and (b) Metf dosage form acquired at 9.4 T and υ_{rot} = 8 kHz. Spinning sidebands are denoted by *.

Discussion:

The peaks at 158 and 160 ppm correspond to the guanidine carbons C(1) and C(2) (**Table S16)**. The methyl carbons, C(3) and C(4), were assigned to peaks at 39 and 40 ppm. Peaks between 55 and 110 ppm are observed in the spectrum of the tablet that correspond to cellulose and starch. The peak at 21 ppm suggests the presence polyvinylpyrrolidone (PVP). The broadening between 170 and 180 ppm could also be signal from the amide carbon of PVP. However, this is not conclusive evidence because the region is poorly resolved due to the low S/N of the spectrum.

Table S16. Carbon chemical shift assignments for Metf.

^{13}C shift assignment	Chemical Shift (ppm)	C type	Source
1	160	guanidine 1	Metf
2	158	guanidine 2	
3	40	methyl 1	
4	39	methyl 2	
A	104	polysaccharide	Excipient
B	74	polysaccharide	
C	21	PVP	

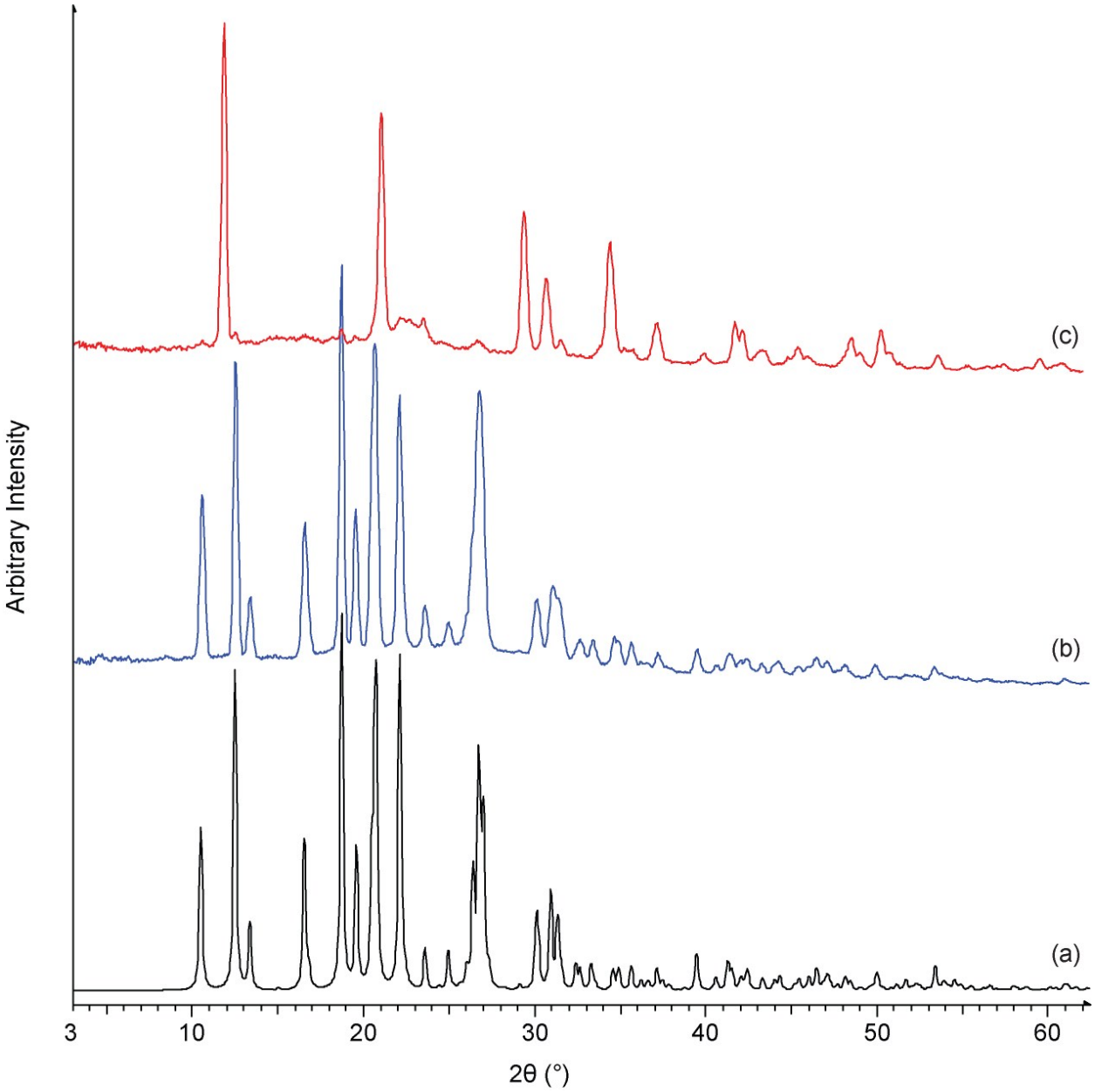

Figure S3. The (a) simulated pattern of the crystal structure of Diph,[4] (b) experimental PXRD pattern of bulk Diph (from Sigma-Aldrich), and (c) experimental PXRD pattern of Diph tablet.

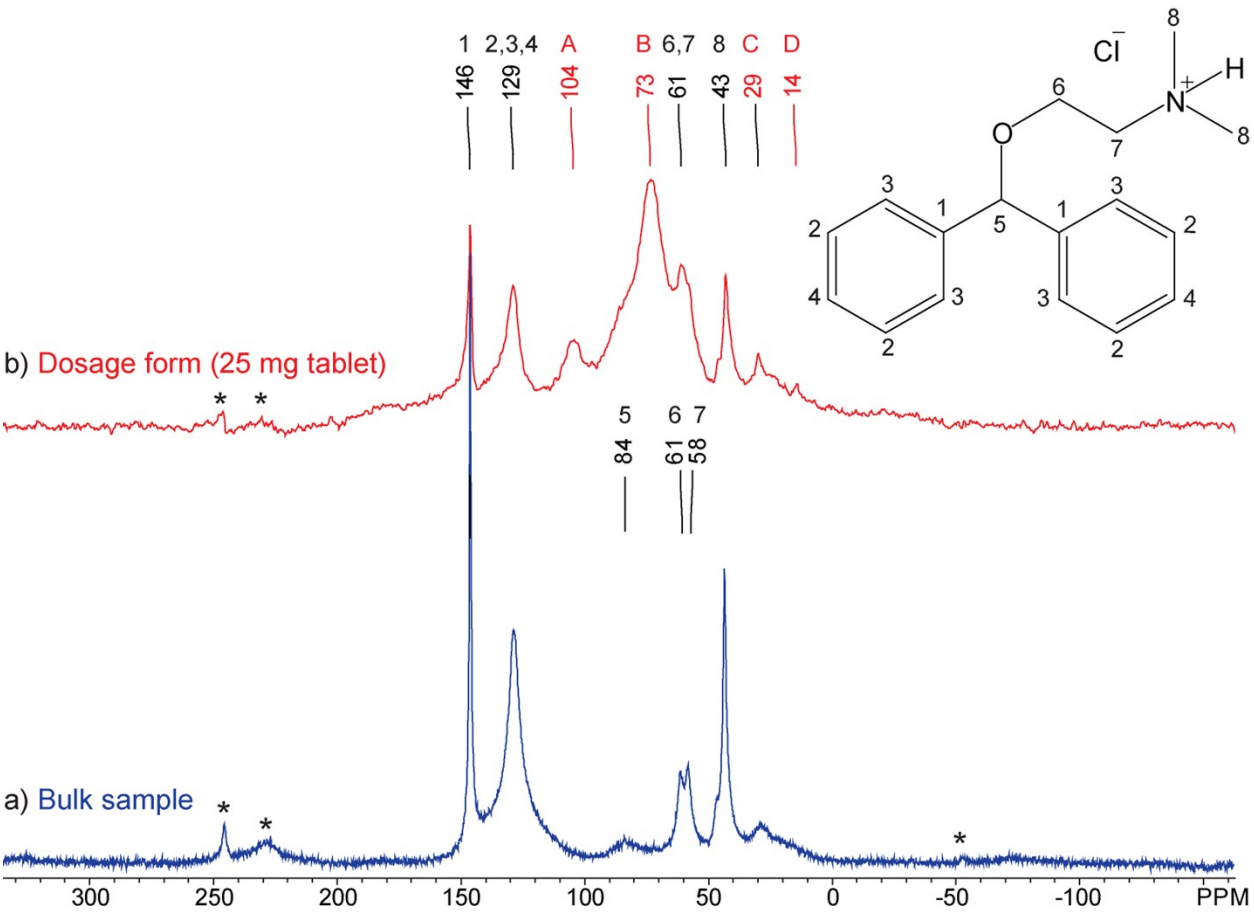

Figure S4. ^{1}H-$^{13}C\{^{1}H\}$ VACP/MAS SSNMR spectra of the (a) Diph (bulk) sample and (b) Diph dosage form acquired at 9.4 T and υ_{rot} = 10 kHz. Spinning sidebands are denoted by *.

Table S17. Carbon chemical shift assignments for Diph.

^{13}C Shift Assignment	**Chemical Shift (ppm)**	**C type**	**Source**
1	146	aromatic	Diph
2, 3, 4	129	aromatic	
5	84	tertiary	
6	61	secondary	
7	58	secondary	
8	43	methyl	
A	104	polysaccharide	Excipient
B	73	polysaccharide	
C	30	polysaccharide	
D	14	PEG	

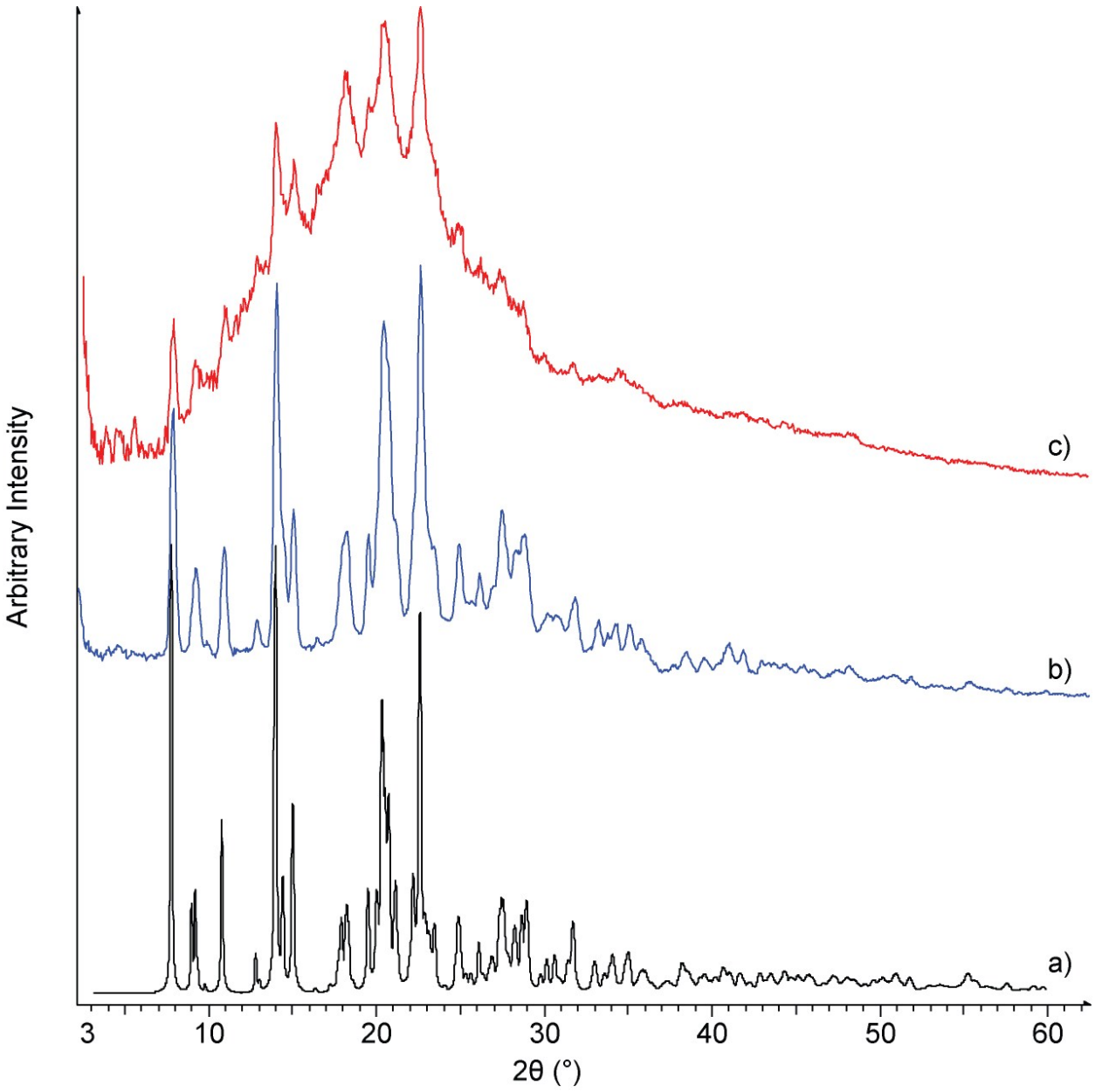

Figure S5. The (a) simulated pattern of the crystal structure of Nica(β),[5] (b) experimental PXRD pattern of Nica (from Sigma-Aldrich), and (c) experimental PXRD pattern of the Nica capsule contents.

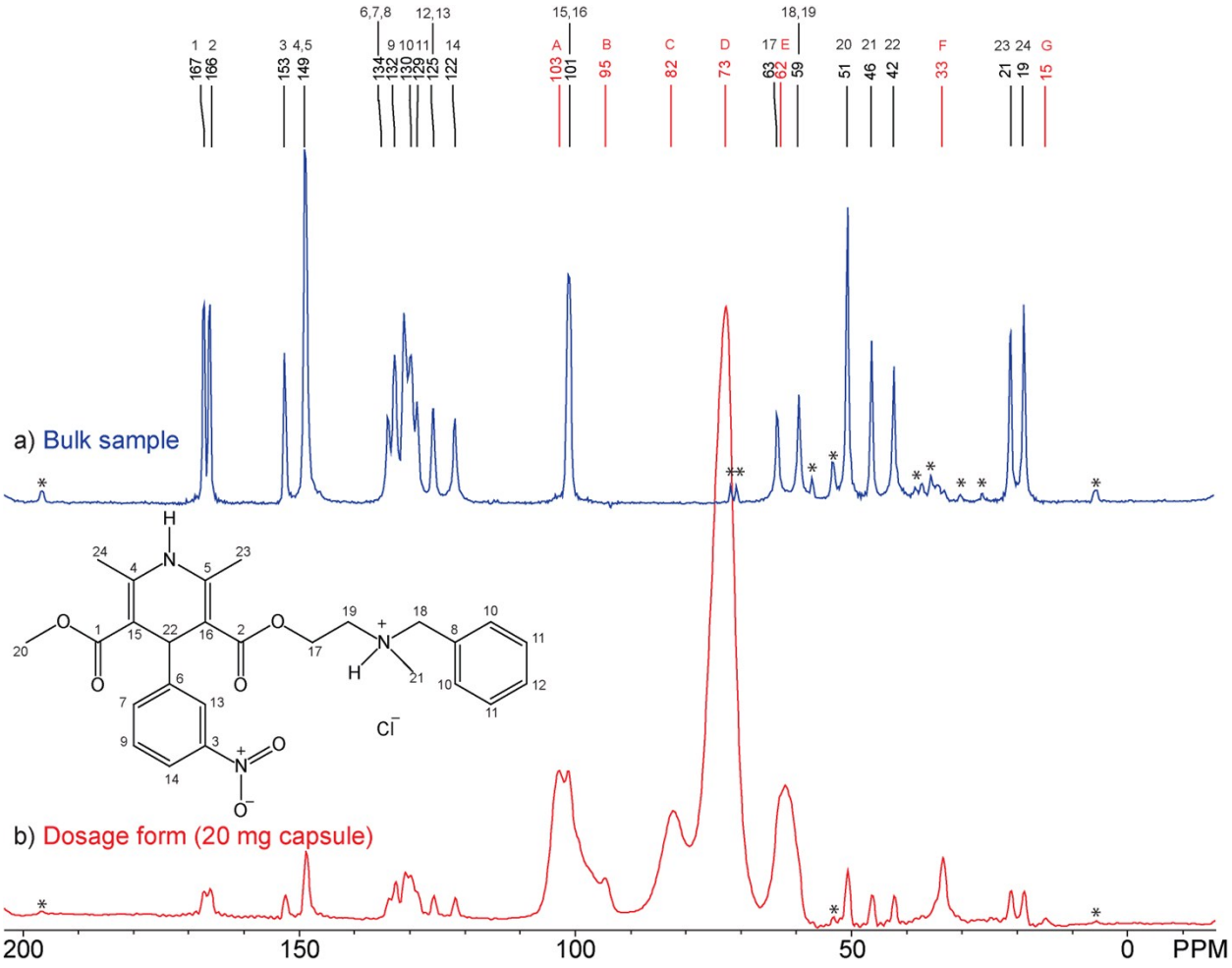

Figure S6. ^{1}H-$^{13}C\{^{1}H\}$ VACP/MAS SSNMR spectra of the (a) Nica (bulk) sample and (b) Nica dosage form acquired at 11.7 T and υ_{rot} = 12 kHz. Spinning sidebands are denoted by *.

Discussion: The resonances at 59 and 63 ppm which correspond to C(17), C(18) and C(19) are obscured in the spectrum of capsule by a broadened excipient peak centred at 62 ppm. Similarly, the C(15) and C(16) peaks are masked by the broadened region spanning 93 to 107 ppm that most likely originates from cellulose derivatives. The peaks at 15 ppm and 33 ppm are assigned to PEG and magnesium stearate, respectively. The excipient peaks are of very high intensity relative to those to the API, which is consistent with the low concentration Nica in the capsule (12.3 %-weight API, **Table S2**).

Table S18. Carbon chemical shift assignments for Nica.

^{13}C Shift Assignment	Chemical shift (ppm)	C type	Source
1,2	166-167	carboxyl	
3	153	nitrosyl	
4,5	149	amino, alkene	
6,7,8	134	aromatic	
9	132	aromatic	
10	130	aromatic	
11	129	aromatic	
12,13	125	aromatic	
14	122	aromatic	Nica
15,16	101	alkene	
17	63	hydroxyl	
18,19	59	amino	
20	51	hydroxyl	
21	46	amino	
22	42	tertiary	
23	21	methyl	
24	19	methyl	
A	103	polysaccharide	
B	95	polysaccharide	
C	82	polysaccharide	
D	73	polysaccharide	Excipient
E	62	polysaccharide	
F	33	magnesium stearate	
G	15	PEG	

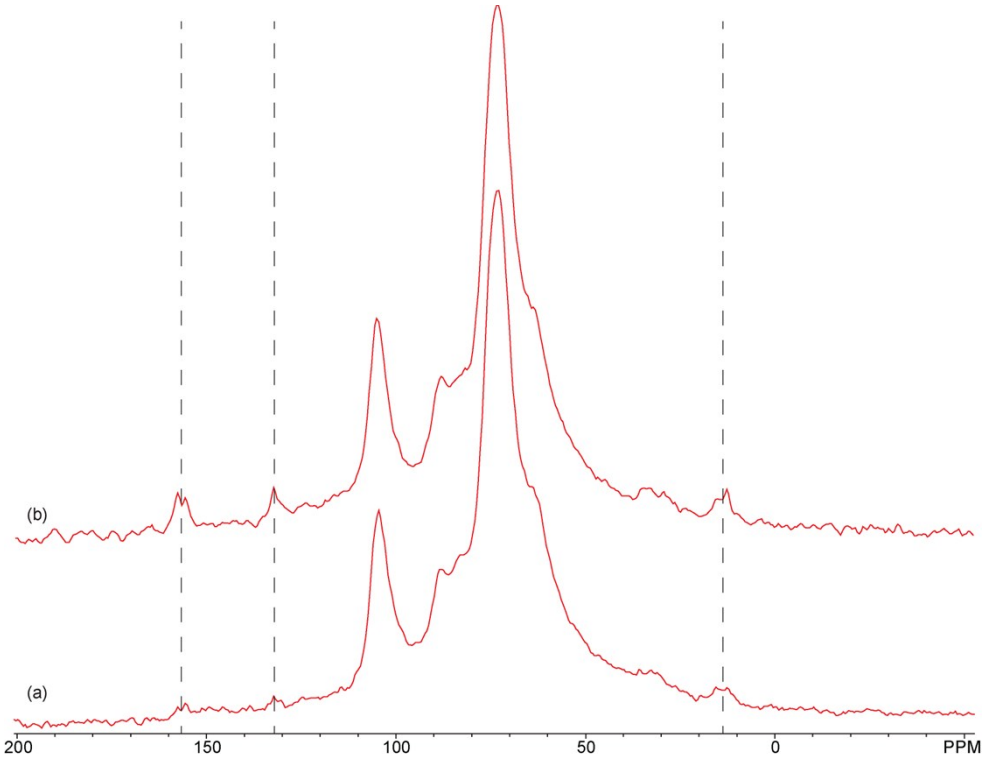

Figure S7. ^{1}H-^{13}C VACP/MAS (9.4 T) SSNMR spectra of the Isox tablet with a contact time of (a) 4.0 ms, and (b) 10.0 ms. υ_{rot} = 13 kHz. Spinning sidebands are denoted by *. Dashed lines indicate observable API signal.

Discussion:

Two peaks at ca. 156 and 157 ppm are visible in the spectrum of Isox-I, whereas only a single broadened peak is observed at ca. 157 ppm in the Isox-II spectrum. Also, two peaks (117 ppm and 112 ppm) in the aromatic region of the Isox-I spectrum are resolved, but absent in the spectrum of Isox-II. The ^{13}C SSNMR spectrum of the Isox tablet is dominated by polysaccharide excipient signal between 100 and 110 ppm, and 50 and 90 ppm.

The aromatic fingerprint region of the API is not observed in the spectrum of the tablet due to low signal intensity. Peaks at ca. 156 and 157 ppm are present in the spectrum of the tablet, suggesting that the polymorph contained in the dosage form is Isox, consistent with the ^{35}Cl SSNMR data.

The optimized contact time for ^{13}C VACP/MAS experiments of the bulk Isox polymorphs was found by Hildebrand *et al*. to be 4.0 ms (**Table S12**).[1] However, the excipients in the dosage form have a similar optimal contact time. Since the S/N ratio of the excipient is severely reduced at higher contact times, but only moderately affected for the API, experiments on the tablet used a contact time of 10.0 ms to suppress excipient signal relative to the API (comparison shown above).

References

(1) Hildebrand, M.; Hamaed, H.; Namespetra, A. M.; Donohue, J. M.; Fu, R.; Hung, I.; Gan, Z.; Schurko, R. W. *CrystEngComm* **2014**, *16*, 7334.

(2) Childs, S. L.; Chyall, L. J.; Dunlap, J. T.; Coates, D. A.; Stahly, B. C.; Stahly, G. P. *Cryst. Growth Des.* **2004**, *4*, 441.

(3) Oh, T. J.; Nam, J. H.; Jung, Y. M. *Vib. Spectrosc* **2009**, *51*, 15.

(4) Glaser, R.; Maartmann-Moe, K. *J. Chem. Soc.-Perkin Trans. 2* **1990**, 1205.

(5) Moreno-Calvo, E.; Munto, M.; Wurst, K.; Ventosa, N.; Masciocchi, N.; Veciana, J. *Mol. Pharm.* **2011**, *8*, 395.